

BEAM CONTROL AND LASER DIAGNOSTIC SYSTEMS

<i>E. S. Bliss</i>	<i>A. A. Grey</i>	<i>R. D. Kyker</i>
<i>F. R. Holdener</i>	<i>R. D. Demaret</i>	<i>T. J. McCarville</i>
<i>J. T. Salmon</i>	<i>C. M. Estes</i>	<i>V. J. Miller Kamm</i>
<i>J. R. Severyn</i>	<i>M. Feldman</i>	<i>R. A. Sacks</i>
<i>R. A. Zacharias</i>	<i>A. J. Gates</i>	<i>C. E. Thompson</i>
<i>S. A. Boege</i>	<i>W. E. Rivera</i>	<i>R. L. Van Atta</i>
<i>R. D. Boyd</i>	<i>C. F. Knopp</i>	<i>S. E. Winters</i>

The beam control and laser diagnostic systems for the National Ignition Facility (NIF) align the laser beam, diagnose the beam, and control the beam's wavefront. Accomplishing these tasks requires approximately 12,000 motors and other actuators, 700 cameras and other detectors, and 192 wavefront sensors and deformable mirrors.

System control components are located throughout each beamline as illustrated in Figure 1. Each of NIF's numerous laser control systems serves one or more of the following three functions: laser beam alignment, beam diagnostics, or wavefront control. We designed many of the systems to perform multiple functions and share components to reduce the costs and space

requirements for NIF. For instance, the input sensors both align and diagnose the initial laser pulse.

The specific requirements for alignment include positioning the 192 beams within the 40-cm apertures of the laser components, focusing them accurately through the far-field pinholes of the amplifier-chain spatial filters, and delivering them to the precise locations specified on the target. All alignment functions are accomplished automatically by recording video images of reference light sources and beams, calculating what adjustments will achieve the desired relative positions of the imaged objects, and sending the corresponding commands to system motors.

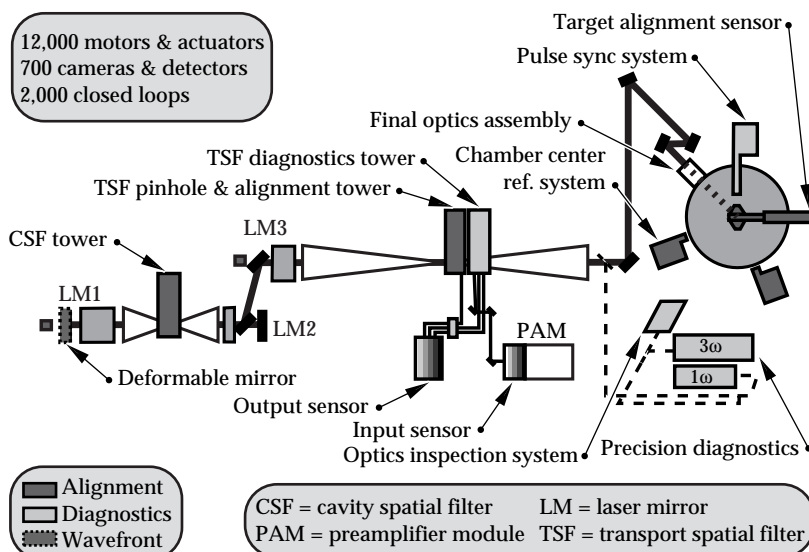


FIGURE 1. Major beam control components for a single NIF beamline. (40-00-1097-2260pb02)

The laser diagnostic systems measure the beam energy, power vs time, and the near-field transverse profile. The detectors that monitor these parameters are calorimeters, fast photodiodes, streak cameras, and charge-coupled device (CCD) video cameras. Requirements for accuracy and reliability are very high.

Wavefront systems measure optical aberrations on the laser output beams and use a deformable mirror in the four-pass amplifier of each beamline to compensate. The resulting improvement in beam quality leads to higher frequency-conversion efficiency and provides better focusing characteristics in the target chamber.

For the sake of clarity, this article is organized by function—laser beam alignment, beam diagnostics, and wavefront control. The input sensor components that handle alignment are described in the laser beam alignment section, whereas the input sensor's diagnostic components are described in the following section on beam diagnostics. Discussion of the front-end processors, another important element of laser control, appears in the "Integrated Computer Control System" article (see p. 21).

Laser Beam Alignment

In the NIF, laser beam alignment is performed in the following areas:

- Input sensor.
- Spatial filter towers.
- Output sensor.
- Target area.

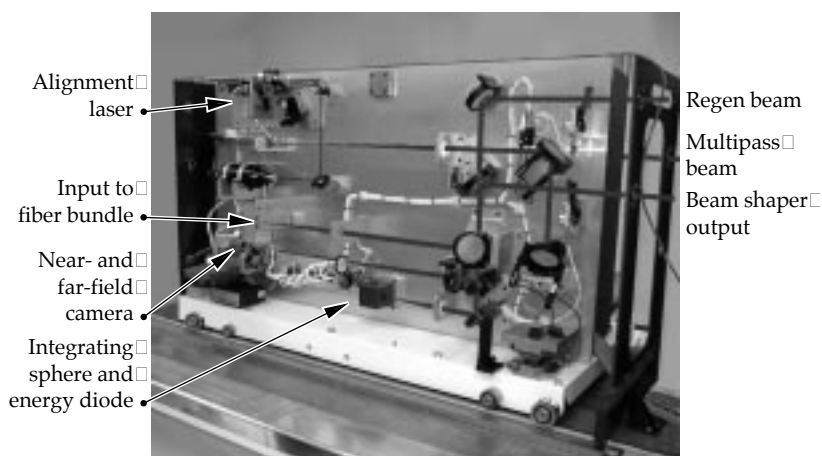
We discuss the design of the alignment components in each of these areas below.

Input Sensor

The input sensor is located at the output of the preamplifier module (PAM) of the optical pulse generator. For alignment purposes, the input sensor must measure beam pointing and centering, provide alignment references, and provide a beam for alignment through the rest of the system. The sensor must monitor the output at three points within the PAM: the regenerative amplifier, the beam shaping module, and the multipass amplifier (for the design of these components, see "The NIF Injection Laser System" article (p. 1). The optical design for this alignment system was driven by three factors: (1) resolution and field-of-view requirements, which are directly related to performance of the sensor's function; (2) cost, which limited the number of optical elements and control points; and (3) space, which required that the sensor package fit within the preamplifier transport-optics design footprint. Figure 2 is a photograph of the instrumentation side of a prototype input sensor with beam paths highlighted. The main beam passes on the other side of the package.

The sensor includes a CCD camera that measures both the near-field and far-field intensity profile of the beams. For the far field, the camera measures beam pointing and provides a pointing reference for the PAM control points. The same camera is used to produce a near-field image for

FIGURE 2. Photograph of a prototype of the NIF input sensor package that is being tested in the laboratory. Instruments and indications of beam paths have been labeled. (40-00-0499-0879pb01)



beam-centering alignment. We designed this camera to perform its near-field imaging without disrupting the far-field pointing reference by adding insertable lenses to the fixed far-field lens element and camera.

The continuous-wave (CW) alignment light source shown in Figure 2 is used to align the rest of the system. It provides a beam of the same wavelength and size as the regenerative amplifier (regen) beam. Although the regen beam itself can also be used, it is not always available between shots, and then only at the rate of one pulse per second. The CW alignment beam goes through the input-sensor beam shaper, where it is shaped into a 27.5-mm-square beam.

Spatial Filter Towers

The spatial filter towers are line-replaceable units (LRUs) that are installed from above at the center of the cavity spatial filter (CSF) and transport spatial filter (TSF) (Figure 3). These towers hold multiple components that serve several functions for each beam, as shown in Figure 4. Platforms holding the components for two beams are mounted at each of the four levels in the towers. They provide a stable base for

injection optics, diagnostic optics, pinhole assemblies, and beam dumps. Figure 5 is a photo of a prototype alignment tower platform with some of the components for one beam mounted. This prototype has been shown to meet precision requirements.

Each platform in the CSF and each alignment platform in the TSF has a pinhole assembly that rotates around an axis parallel with the beam propagation direction to accurately position one of the multiple sets of pinholes in the focal plane of the corresponding spatial filter lenses. The same platforms also carry pointing references to which the alignment beam from the input sensor is aligned between shots. In the CSF, the reference takes the form of a reticle that is positioned by selecting a particular position of the rotating pinhole assembly. A local illuminator, also mounted on the platform, provides light for viewing the reticle directly with a camera on the same platform. In the TSF, as shown in Figures 4 and 5, the pointing references are provided by fiber-optic light sources moved into the pinhole plane by their own precision translation stage. Images of the TSF references are viewed in the output sensor. Baffles, one of which is shown in Figure 5, control stray light. Fixed and prealigned beam dumps absorb energy

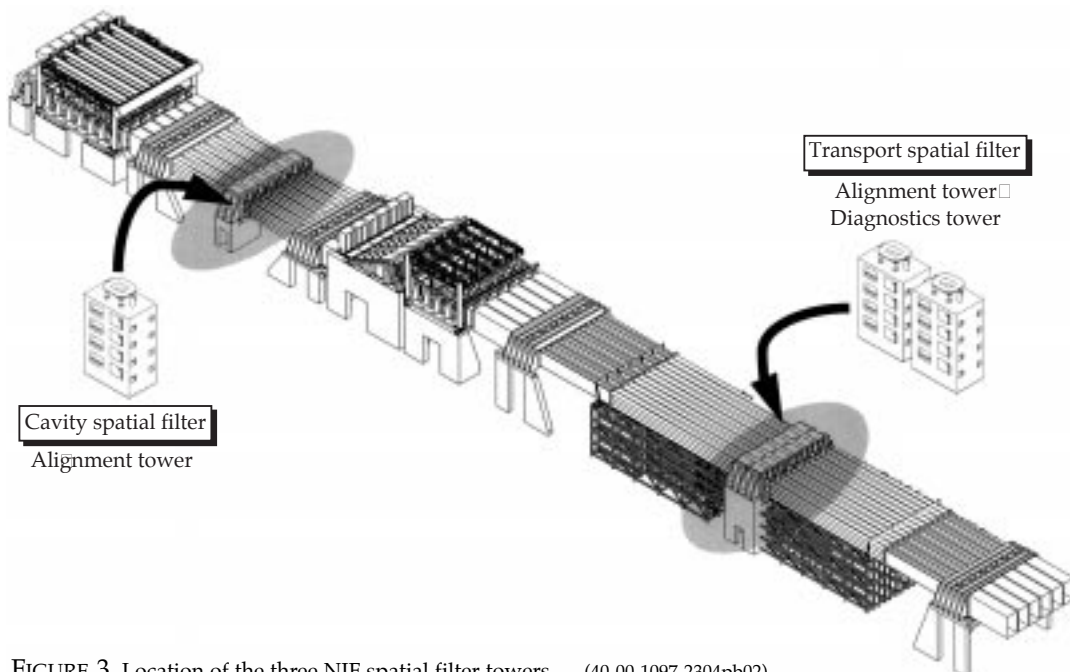
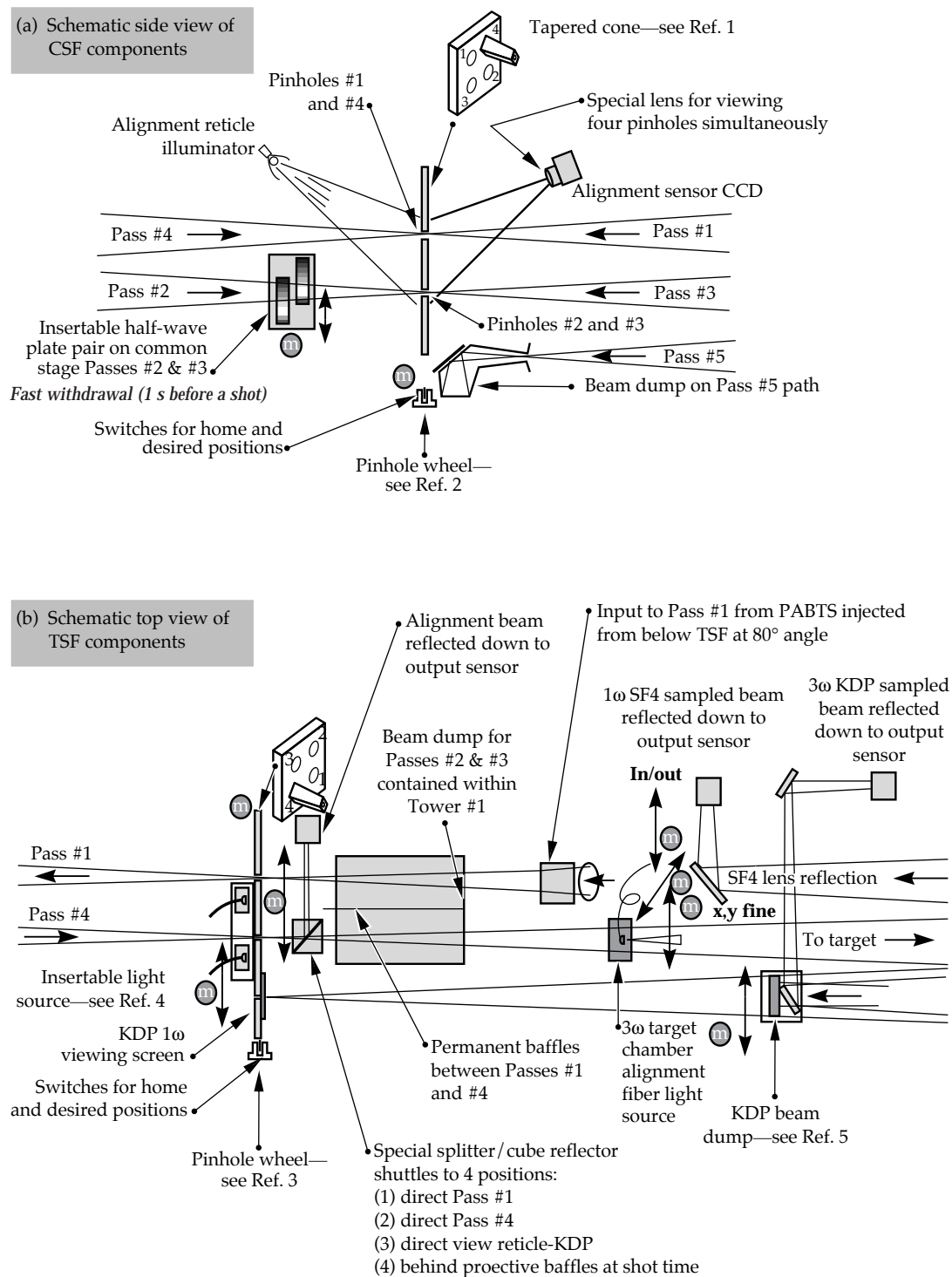


FIGURE 3. Location of the three NIF spatial filter towers. (40-00-1097-2304pb02)

FIGURE 4. Schematic views of the (a) CSF tower and (b) TSF alignment and diagnostic tower components for one beam.
(40-00-0499-0880pb01)



from faults or leakage from the Pockels cell and from target back reflections. The pointing references and other alignment optics identified in Figure 4 are removed from the beam path to fire the laser.

Output Sensor

The output sensor and relay optics packages are located beneath the TSF center vessel, as shown in Figure 6. The sensor



FIGURE 5. A prototype alignment tower platform with the principal components for one beam. (40-00-0499-0881pb01)

and relay optics view the following, for alignment purposes:

- Injection beam at Pass 1 for injection pointing.
- Pass 1 in near field for beam centering at the final optics.
- Pass 4 in far field for output pointing.
- Pass 4 in near field for beam centering.
- Reflection from the final optics at the pinhole plane to adjust the angle of the KDP frequency conversion crystals.

These systems are required to center beams within 0.5% of the beam dimension, locate the focused beams on shot pinholes within 5% of the pinhole diameter, position beams on target within 50- μm rms, and adjust the KDP crystal angle within $\pm 10\ \mu\text{rad}$ over a field of view of $\pm 200\ \mu\text{rad}$. Light for these tasks is intercepted by a moving beam-splitter cube pickoff near the TSF pinhole plane on the alignment tower (see Figure 4b).

Light for all these functions is then directed down to the output sensor along a single path per beam. The pickoffs, relay optics, and transport mirrors are staggered to multiplex the eight beams spatially for each bundle. Two beams per bundle “time share” each output sensor, using beam splitters and shutters in the transport paths. The nominal beam size in the relays is 20 mm.

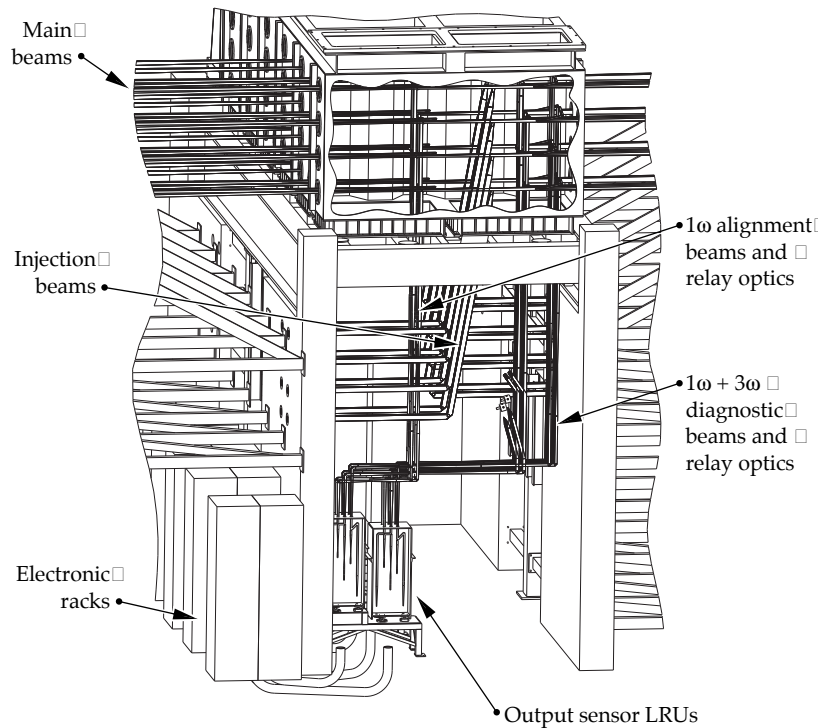


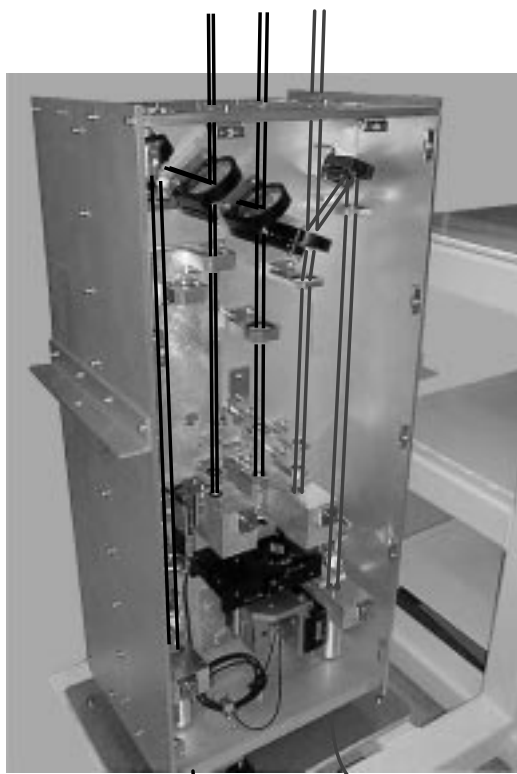
FIGURE 6. The output sensor packages and associated relay optics are located below the center part of the TSF. (40-00-1097-2249pb02)

Figure 7 is a photograph of the prototype NIF output sensor package with beam paths added for illustration. Only the 1ω camera is used for alignment. It has two lens systems for near-field and far-field viewing and a motorized focus adjustment. The near-field lens system is shared with diagnostics (see the diagnostics discussion on p. 85), and the far-field lens system performs focused beam and reticle viewing functions. Both cameras have motorized continuously variable attenuators.

Target Area

We have two main alignment systems in the NIF target area: the chamber center reference system (CCRS) and the target alignment sensor. Figure 8 shows the layout of these two systems within the target chamber. The target alignment sensor inserter uses the same positioner design as the target inserters. These inserters, the CCRS modules, and target diagnostics are mounted on the same platform to minimize the relative motion among them. At

FIGURE 7. This photograph shows the principal components and beam paths of the prototype NIF output sensor package being tested in the laboratory. The output sensor performs both alignment and diagnostic functions. (40-00-0499-0882pb01)



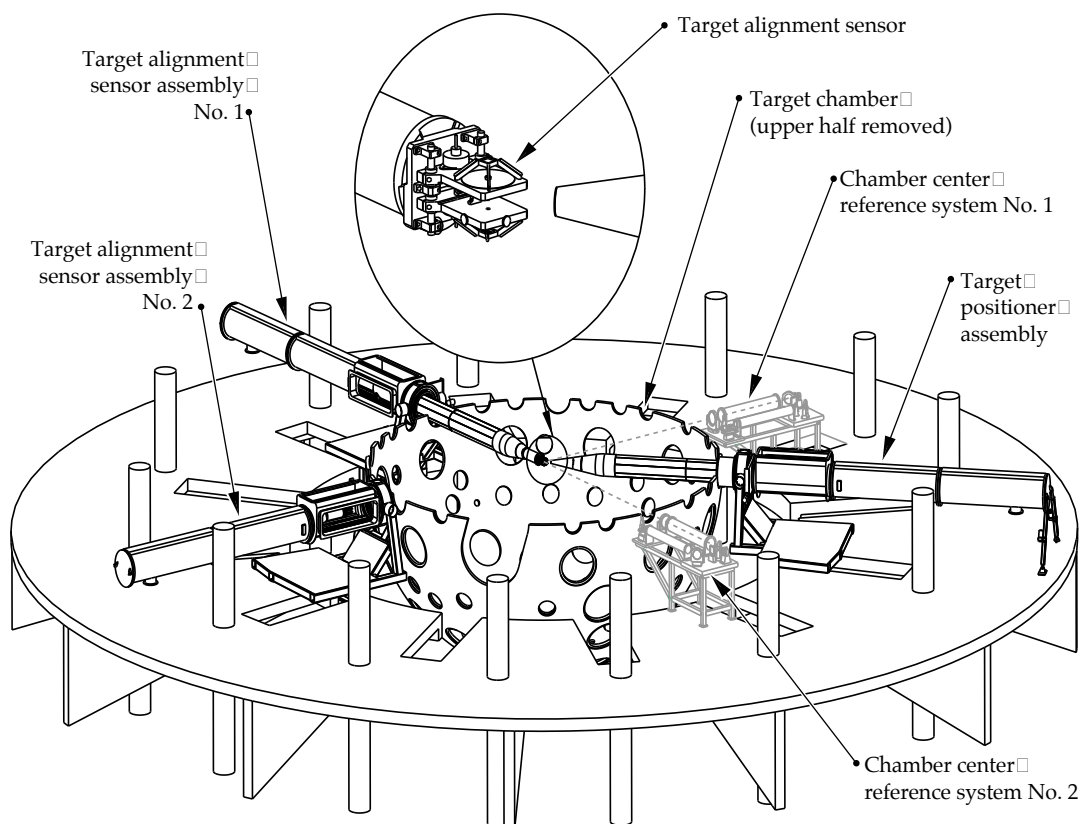
shot time, the alignment sensor is removed and protective baffles are positioned in front of the CCRS port windows.

The CCRS must provide a stable position reference system in the target bay and be able to position targets repeatably within the narrow field of view (FOV) of the target diagnostics. Its long-term stability must be $\leq 30 \mu\text{m}$, and its FOV must be $\pm 5 \text{ cm}$ from the target chamber's center.

The system has two identical viewing instruments that have been adjusted to identify a common position in the center of the target chamber, and each has two simultaneous modes of operation. One mode measures a component's target chamber position by imaging the position of a reticle on the component. The other mode measures the component's orientation by monitoring the direction of light reflected from the reticle.

The target alignment sensor collects images of alignment beams in the target plane and provides data for controlling beam

FIGURE 8. Layout of the target area alignment systems. (40-00-1097-2251pb02)



positions and spot size. The total deviation for all beams must be $\leq 50 \mu\text{m}$ rms; a single beam must deviate no more than $200 \mu\text{m}$; and the sensor must achieve a specified central lobe size to $\pm 50 \mu\text{m}$. The sensor must operate everywhere within 5 cm of the target chamber center. Figure 9 shows a schematic of the setup for the target alignment sensor and a photo of the prototype. The sensor has two CCDs, which see both the target and the beams. The assemblies that reflect the beams were designed for minimal deflection and high natural frequency.

Beam Diagnostics

NIF's beam diagnostics characterize the beam at key locations in the beamline (Figure 10). These systems include the:

- Input sensor.
- Output sensor.
- Calibration calorimeters and final optics diagnostics.
- Temporal diagnostics.
- On-line optics inspection system.
- Target chamber diagnostics.
- Supplemental diagnostics:
 - Roving assemblies.
 - Trombones.
 - Precision diagnostics.

We briefly discuss the requirements and design activities of each of these diagnostic systems below.

Input Sensor

The input sensor, in addition to providing certain alignment functions (see p. 80

and Figure 2), characterizes the PAM by sampling at the output of the regenerative amplifier, the beam shaping aperture, and the multipass rod amplifier. The sensor measures beam energy, near-field images, and temporal pulse shape. The imaging resolution is 1% of the beam dimension and 2% of the maximum fluence.

Diagnostic samples are obtained from a 1% partial reflector for the regenerative amplifier and through leaky mirrors for the beam shaper and multipass amplifier. The coatings on these mirrors provide adequate signal levels to the energy diagnostics, as well as to the alignment diagnostics.

The energy from the regen, beam shaper, or four-pass amplifier is measured with an integrating sphere and photodiode followed by a charge integrator and digitizer. Shutters select which sample is measured and a CCD camera obtains near-field images for each beam prior to or during a shot. An optical fiber bundle sends a sample of the multipass output to the power sensor (see Figures 10 and 13), where it is time multiplexed with other signals. The PAM output beam can also be diverted to a calorimeter to periodically calibrate the multipass energy diagnostic.

Output Sensor

The output sensor performs many diagnostic tasks in addition to its alignment functions (for alignment discussion, see p. 82). The sensor characterizes the 1ω output (energy, near-field fluence profile, temporal pulse shape, and wavefront) and 3ω output (near-field fluence profile and temporal pulse shape). The 1ω output energy

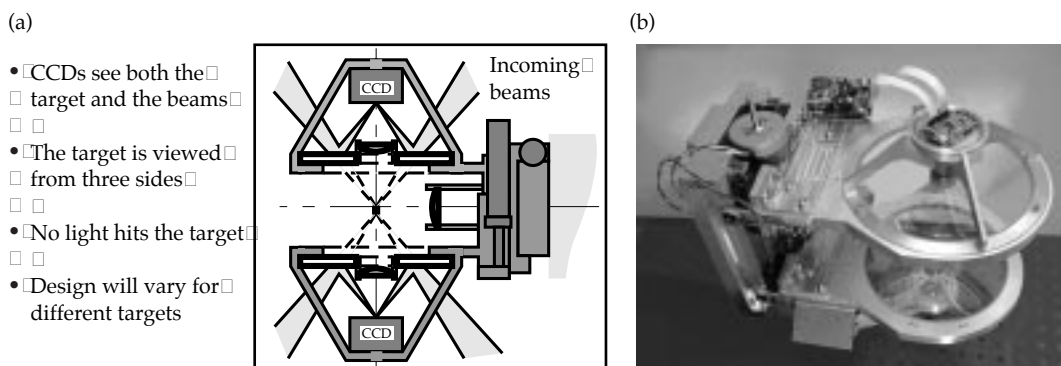
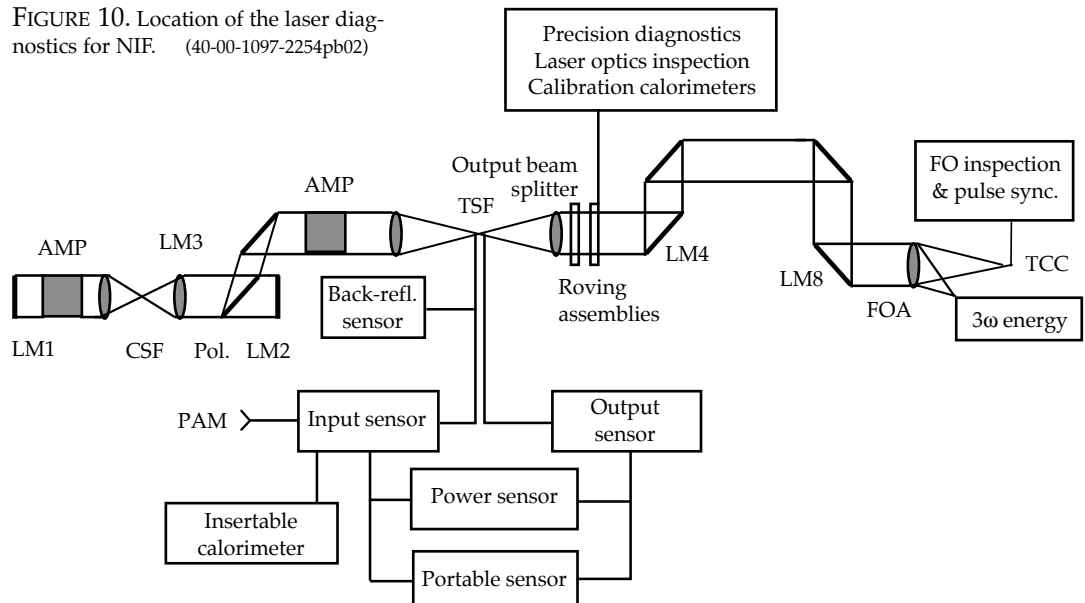


FIGURE 9. (a) A schematic illustrating the setup concept for target alignment. (b) Photograph of the prototype target alignment sensor currently under test. (40-00-0499-0883pb01)

FIGURE 10. Location of the laser diagnostics for NIF. (40-00-1097-2254pb02)

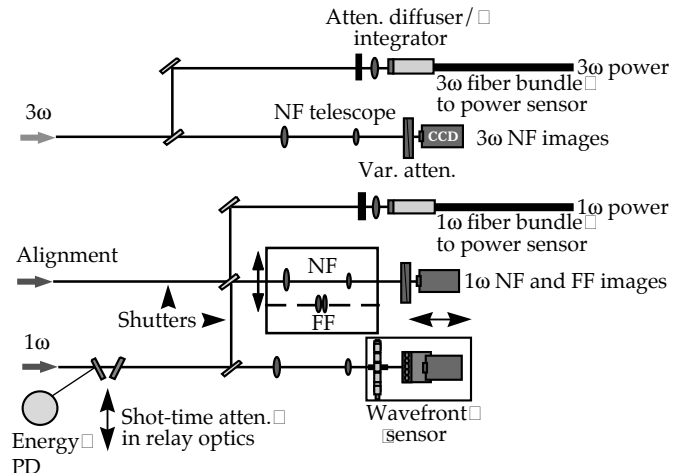


must be measured within 3%, and the 1ω and 3ω temporal pulse shape must be measured within 2.8%. The 1ω beam wavefront must be measured within 0.1 wave, and the 3ω output beam must be imaged at the plane of the conversion crystal with a spatial resolution of 3.2 mm. Figure 7 shows the output sensor's principal components and beam paths, and Figure 11 shows a schematic for the output sensor's diagnostic functions.

Reflections from optics in the main beam supply samples of the 1ω and 3ω beams. The 1ω sample reflects from the front

surface of a beam splitter at the output of the TSF. This surface is coated with a solgel antireflection coating (nominally 0.1% R), and the splitter is tilted by 0.8 mrad to offset the reflected sample from the path of the existing beam. The 3ω sample reflects from the flat entrance surface of the target chamber lens in the final optics assembly. This lens is also tilted by 0.6 mrad to the opposite side to offset the reflected sample beam from the exit path, and its coating is similar to that on the SF4 lens sampling surface. Pickoffs for the beam samples are near the focus in the TSF. Pickoff optics for

FIGURE 11. Output sensor schematic for beam diagnostics. NF and FF mean near field and far field, respectively. PD means photodiode. (40-00-1097-2256pb01)



1ω and 3ω sample beams are located on TSF Tower #2, as shown in Figure 4. Relay optics transport the beams from the TSF to the output sensors beneath the TSF center vessel. Each side of the output sensor collects data for two beams as illustrated in Figures 7 and 11.

The output sensor has three CCD cameras, each with continuously variable attenuators. One camera—shared with the alignment functions—images the 1ω near-field profile, the second images the 3ω near-field profile, and the third is the detector array for a Hartmann wavefront sensor (see p. 93 for a discussion of the Hartmann sensor). The 1ω energy is measured by an integrating sphere with a time-integrated photodiode, which is inserted at shot time. Power samples are sent to the power sensor (see Temporal Diagnostics at right column) using two optical fiber bundles.

Calibration Calorimeters and Final Optics Diagnostics

Calorimeters, which measure beam energy, are used in three areas of NIF: the input sensor, the output sensor, and the final optics diagnostics. Each input sensor has a port for manual mounting of a 5-cm calorimeter to calibrate the sensor's energy diode without opening the beamline (Figure 2). The output energy diodes are calibrated using two groups of eight roving bundles of 50-cm calorimeters—one for each laser bay. Each group can be remotely positioned to intercept the outputs from one eight-beam bundle at a

time. Finally, 192 10-cm calorimeters in the final optics diagnostics measure a fraction of each beam's 3ω energy as it propagates toward the target.

We use calorimeters similar to those on Nova. The 5-cm calorimeters are an off-the-shelf design, and the 50-cm and 10-cm calorimeters are scaled versions of the 40-cm ones used in the Nova target chamber. These calorimeters can meet the NIF requirements.

The final optics diagnostics uses a diffractive splitter to obtain a sample for the 3ω calorimeter (Figure 12). This calorimeter calibrates the 3ω power for each shot. It must operate in a vacuum, and have a damage threshold $>3 \text{ J/cm}^2$ at 351 nm, a $10\text{-} \times 10\text{-cm}$ aperture, a 1- to 60-J energy range, a repeatability of $<1\%$ at the 30-J level, and a linearity of $<1\%$ over a range of 50:1. The sampling grating on the flat surface of the focus lens diverts $<1\%$ of the 3ω energy and focuses the sample in front of the calorimeter.

Temporal Diagnostics

Temporal diagnostics includes two portable sensors, rack-mounted power sensors near the input and output sensors, and a back-reflection sensor. NIF will have two portable streak cameras, mounted on carts, which can each be used in place of a normal power sensor for one beam at a time. The streak cameras must have a time resolution of 10 ps, a dynamic range of 1000:1, and multiple channels, and be easily movable among the other sensor packages. Each camera

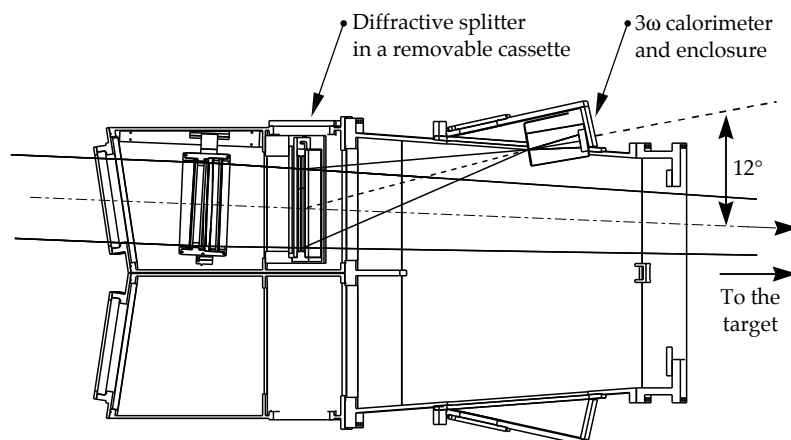


FIGURE 12. The final optics diagnostics uses a diffractive splitter and volume-absorbing calorimeter. (40-00-1097-2257pb02)

can handle 19 sample inputs— 1ω or 3ω —through fiber-optic bundles. One of four sweep times can be selected—1.5 ns, 5 ns, 15 ns, or 50 ns—with resolutions from 10 ps (for 1.5 ns) to 250 ps (for 50 ns).

Each power sensor must have a dynamic range of 5000:1, a record length of 22 ns, an accuracy of 2.8% averaged over a 2-ns interval, and a rise time of 450 ps. It takes samples on fiber bundles from the output and input sensors, and time multiplexes signals as shown in Figure 13 to minimize costs. The transient digitizer in the sensor is a commercial technology with a long record length. Each 1ω photodiode receives signals from four input sensor fiber bundles and eight output sensor fiber bundles. Each 3ω photodiode receives signals from four output sensor fiber bundles. Time separation is achieved using the propagation time through the laser and optical fiber delay lines for signals close in time. The dynamic range of the eight-bit digitizer is extended using four channels, each with a different sensitivity.

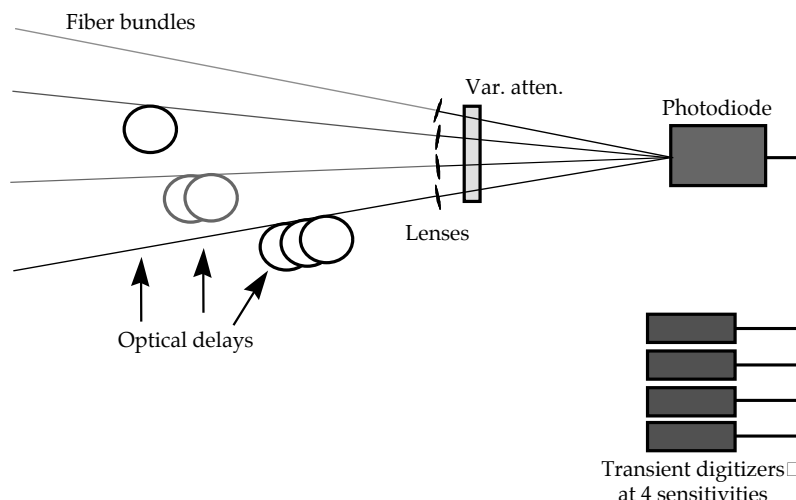
On-Line Optics Inspection System

One on-line optics inspection system is located in each switchyard, and one more at target chamber center. These systems have access to each beamline through a set of translatable mirrors described later (see Supplemental Diagnostics on p. 90). The

requirement for main-beam optics is to detect flaws ≥ 3 mm. Our goal is that these systems detect defects ≥ 0.5 mm so that the optics can be removed for refinishing while defects are still small. We considered a number of issues when designing these systems. First, we selected dark-field imaging since damage spots appear best against a dark background. This allows us to detect spots below the resolution limit. Our imaging scheme is to backlight the large optics with apodized and collimated laser illumination sources. Undisturbed light is intercepted by a stop in the dark-field optics, but light diffracted from damage spots is imaged onto a CCD camera. Second, the systems' resolution will be limited by one of two factors: the far-field aperture in the TSF or the number of pixels in the cameras' CCD arrays. We must properly account for these limitations in the design. Third, depth of field will be short enough to isolate all but the most closely spaced optics. Fourth, use of different pinhole combinations in the CSF and careful image processing can "strip away" any overlaid images.

The laser bay optics are inspected with the high-resolution cameras located in each switchyard. Figure 14 shows the layout of a switchyard inspection package. For optics in the main laser, the illumination source is the alignment laser located in the input sensor. This alignment beam is injected into the TSF along Pass 1, and LM1 is aligned to return the beam along Pass 4.

FIGURE 13. Schematic diagram of a power sensor in which time-multiplexed optical pulses are combined on a common photodiode, and the electrical outputs drive multiple channels in transient digitizers. (40-00-1097-2258pb02)



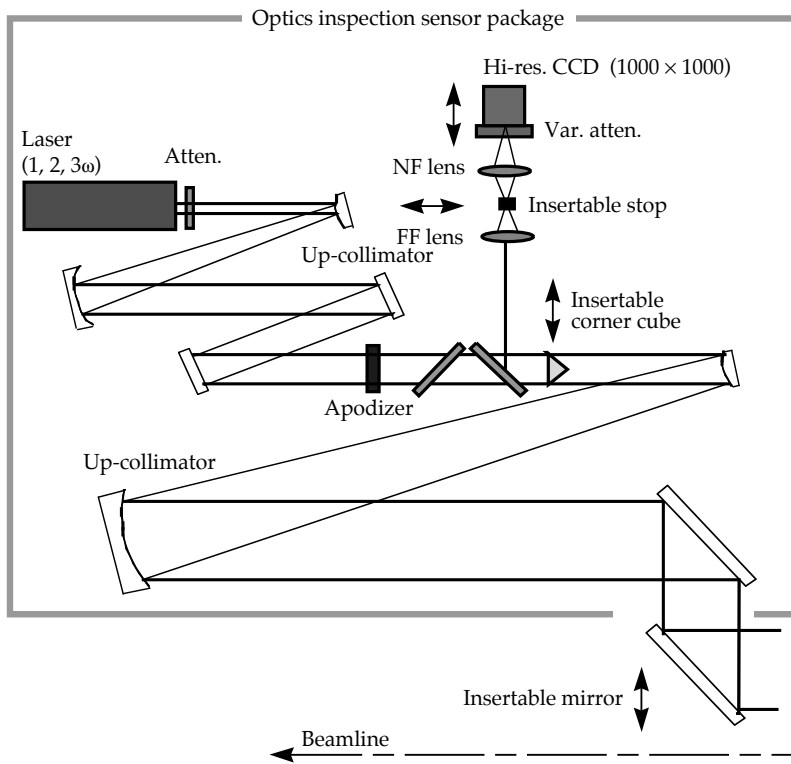


FIGURE 14. Inspection package used for all but the final optics. One such inspection system resides in each switchyard. NF and FF mean near field and far field, respectively. Light is directed into or from the package by an insertable mirror. (40-00-1097-2259pb02)

The inspection package captures dark-field images at each plane containing an optic. Image subtraction software will help detect the changes from previous inspections.

For inspecting switchyard and target optics up to the first surface of the final focus lens, the switchyards' 1ω source will be injected toward the target using the outward-looking roving mirror (p. 91). The first surface of the final focus lens will be aligned to retroreflect a portion of this beam. Dark-field images will be captured by the inspection system in the switchyard at each plane containing an optic.

For inspecting the final optics, we will image through the kinoform phase plate at 3ω using a damage inspection package inserted at the target chamber center (described further in the next section). This viewer will have a sufficiently short depth of field to discriminate between the closely spaced final optics elements.

Target Chamber Diagnostics

Target chamber diagnostics include the pulse synchronization detector module and the target optics inspection system. Both are

located at the center of the target chamber at the end of the diagnostic instrument manipulator, as shown in Figure 15a. Similar adjustments are required for both the pulse synchronization and final optics inspection modules. They can be oriented to any beam position. Translation commands for the diagnostic manipulator and angle commands for the modules come from the CCRS (see Target Area on p. 83). The maximum move time to intercept light from a different four-beam quad is 5 s; the typical time is <0.8 s.

Figure 15b shows the components of the synchronization module. The pulse arrival times at target chamber center must be set with 20-ps relative accuracy. The module must simultaneously capture signals from the four beams of a final optics assembly quad and position each focused beam on the end of a separate fiber bundle with an accuracy of $<100\ \mu\text{m}$. The fiber bundles carry the optical signals to a streak camera where their relative times of arrival are compared. The signal is obtained by firing a rod shot and capturing the leakage of 1ω radiation through the conversion crystals.

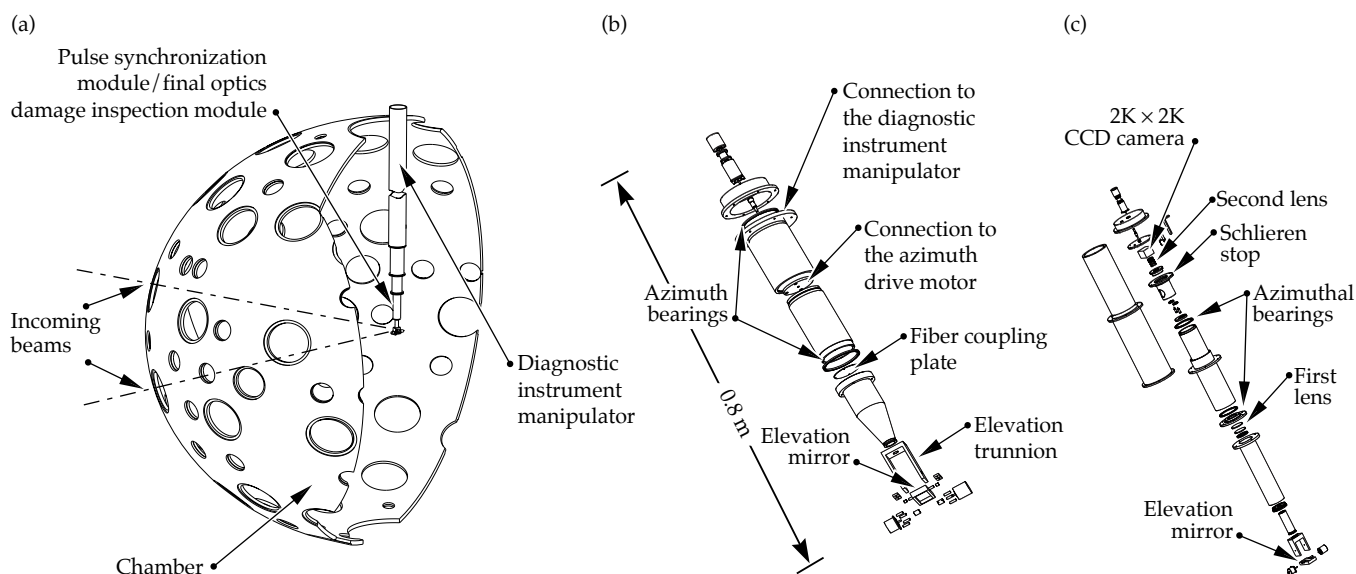


FIGURE 15. (a) The pulse synchronization detector module and final optics damage inspection module can be attached to the end of the diagnostic instrument manipulator and inserted into the center of the target chamber; (b) exploded view of the pulse synchronization module; (c) exploded view of the final optics damage inspection module. (40-00-1097-2261pb02)

The final optics damage inspection module, also located at target chamber center, is shown in Figure 15c. The module examines the closely spaced final optics that are not observable by other means. The final optics are backlit with collimated 3ω radiation. A high-pass filter, with a central schlieren stop placed at the focus, removes those rays that are not deviated by flaws. A CCD camera captures data from the full-aperture image. The camera, lenses, schlieren stop, and filters rotate as a unit in the azimuthal direction.

Supplemental Diagnostics

As described above, the NIF design includes significant diagnostic capabilities on each beamline. However, it will be important to be able to calibrate some of these measurements, to verify that they are operating correctly, or to collect more detailed information. For this purpose, additional diagnostics that can be used on one or a few beams at a time are located in each switchyard. They include full-aperture calibration calorimeters and a suite of precision diagnostics.

Figure 16 shows the layout of components related to supplemental diagnostics in one of the switchyards. An array of

eight calorimeters, the “roving calorimeter assembly,” travels on horizontal rails to any of the 12 bundle locations. If desired, each of the eight calorimeters can collect the output from the corresponding beam in that bundle. However, any of the eight calorimeters can also be rotated toward the laser on its outside vertical edge so that it allows the beam to pass. Beams that are allowed to pass continue on to the target chamber or are directed to the precision diagnostics as described below.

The optical-mechanical system designed to intercept any one beam in each switchyard and send it toward the precision diagnostics is called the “roving mirror system.” It comprises an additional pair of parallel horizontal rails, two pair of parallel vertical rails, and three translatable mirrors. The x-y top mirror (Figure 17a) in combination with the y mirror picks off a beam and diverts it toward the precision diagnostics and optics inspection package. The x-y bottom mirror, combined with the y mirror, provides a path from the optics inspection package to the target chamber (Figure 17b). Both roving systems are inside of a large enclosure through which the laser output beams pass.

Each of the roving calorimeter and x-y mirror assemblies weighs about 1000 lb. The horizontal motion of the assemblies is

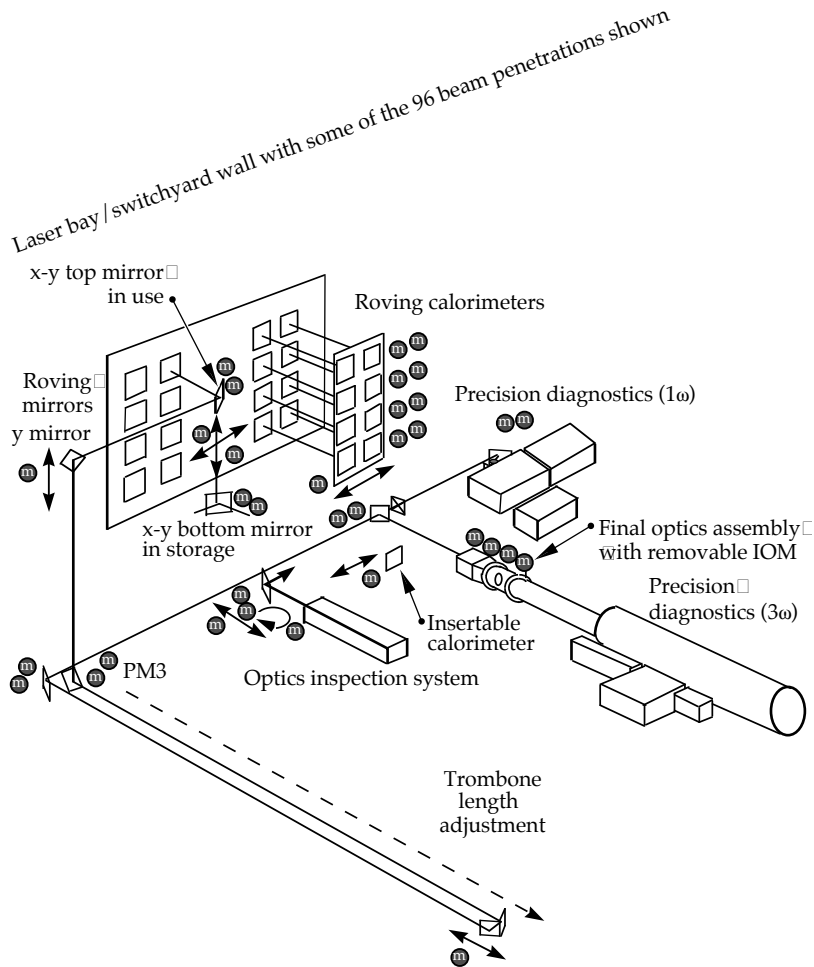
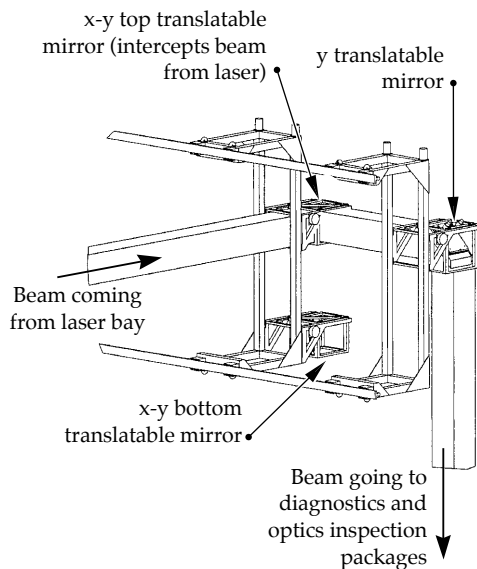


FIGURE 16. Supplemental diagnostics for calibration and for a variety of detailed measurements are located in the switchyard.
(40-00-1097-0381pb02)

(a) Laser bay to precision diagnostics



(b) Inspection diagnostics to target chamber

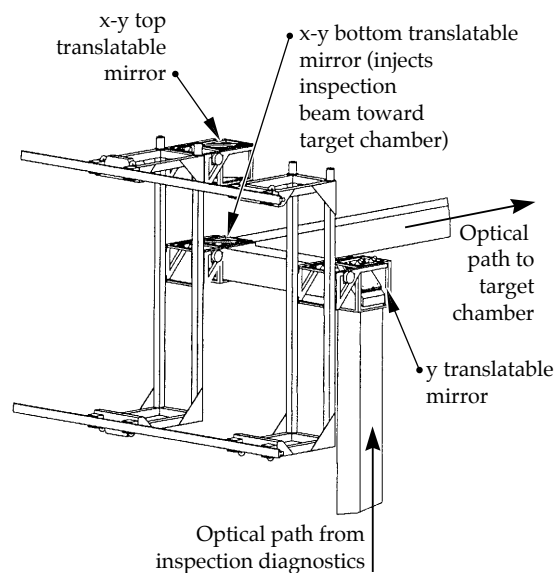


FIGURE 17. Two roving mirror system configurations provide (a) a path from the laser bay to the precision diagnostics station and (b) a path from inspection diagnostics to the target chamber.
(40-00-1097-2262pb03)

belt driven by motors fixed at one end of the enclosure. The average time to move from one beam to an adjacent beam is estimated at 16 s. The enclosure maintains an argon gas environment, and the mechanisms must be designed to avoid production of particles that might contaminate the nearby optics. The path length from the roving mirror to the precision diagnostic stations for each beam is matched to that beam's path length to the target chamber by adjustment of an optical "trombone."

The precision diagnostic stations are shared diagnostics that measure laser output performance one beam at a time using more extensive instrumentation than that found in the output sensors (Table 1). During installation and activation, the precision diagnostics will be used to verify the performance of each beam, including its dedicated diagnostic packages. The 3ω precision diagnostics, illustrated in Figure 18, will measure frequency conversion characteristics of the selected beam using a separately selected integrated optics module (IOM). Each IOM comprises the set of optics, including frequency conversion crystals and final focus

lens, that is normally mounted at each beam's entrance to the target chamber. The precision diagnostics provide the only capability for simultaneously measuring high-power 3ω beam properties at the full 40-cm near-field aperture and in a far-field plane equivalent to the target chamber focus. Once NIF is operational, the station will be available for diagnosing beamline and component problems and for performing laser science experiments.

The precision diagnostic station will be able to measure the following aspects of the 3ω laser pulse:

- Energy, with an accuracy of 2.7%.
- Power vs time, with an accuracy of 3.1% and a rise time of 450 ps for all parts of a 22-ns pulse having a 50-to-1 contrast ratio.
- Focused spot size and smoothness, with 30- μm spatial resolution and 20-ps temporal resolution for a selected 1.5-ns period.
- Near-field spatial profile in the frequency conversion crystal plane, with resolution as high as 300 μm .

TABLE 1. The 1ω measurement capabilities of the precision diagnostic station compared to those of the output.

Measurement	Precision diagnostic	Output sensor
Energy		
Range	To 22 kJ	To 22 kJ
Accuracy	Better than 1.5%	3%
Power resolution	<40 ps or 100 ps	450 ps
Far-field imaging FOV	$\pm 180 \mu\text{rad}$ (best)	None
Near-field imaging resolution (in main beam)	$\sim 1.4 \text{ mm}$ and/or $\sim 300 \mu\text{m}$	3.2 mm
Wavefront		
Hartmann precision	Better than $\lambda/20$	$\lambda/10$
Radial shearing interferometer precision	-0.1λ (16 \times reference)	None
Schlieren		
Energy balance	Better than 15%	None
Power resolution	<40 ps or 100 ps	None
Far-field imaging FOV	$\pm 500 \mu\text{rad}$	None
Near-field imaging resolution	$\sim 1.6 \text{ mm}$ (in main beam)	None
Prepulse sensitivity	$2 \times 10^4 \text{ W/beam}$ for 200 ns preceding foot pulse	None
Potential added measurements	Versatile	Fixed

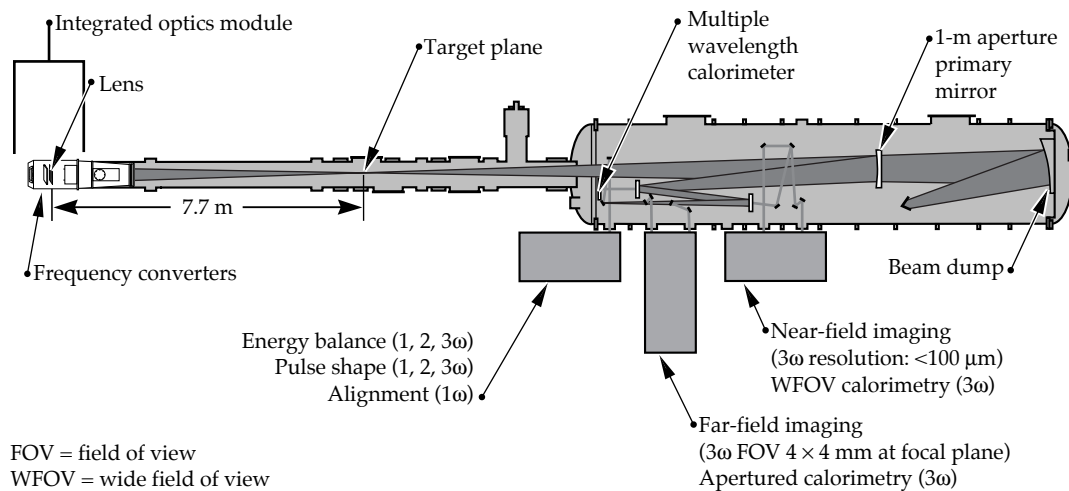


FIGURE 18. The precision diagnostics measure the characteristics of a full-power NIF beamline. The larger vacuum chamber is necessary to avoid high-intensity air breakdown and to expand the beam enough that it doesn't damage beam-splitting optics.
(70-00-0796-1536pb02)

Wavefront Control

The three main components of the wavefront control system are the:

- Hartmann wavefront sensor.
- Deformable mirror.
- Computer controller.

The use of lasers as the driver for inertial confinement fusion experiments and weapons physics applications is based on their ability to produce high-energy short pulses in a beam with low divergence. The focusability of high-quality laser beams far exceeds that of alternate technologies, and the challenge for NIF is to ensure that the potential of high output beam quality is realized. Although considerable effort has been expended to minimize aberrations due to beamline components, other design constraints, including cost, have caused the residual error to be significant. A wavefront correction system is required to compensate for these errors.

During preparations for a pulsed shot, the wavefront control system monitors the wavefront of each alignment laser at the beamline output and automatically compensates for measured aberrations using a full-aperture deformable mirror. In the last few minutes before a shot, the controlled wavefront is biased to include a precorrection for the estimated dynamic aberrations caused by firing the flashlamp-pumped amplifiers. One second before a shot,

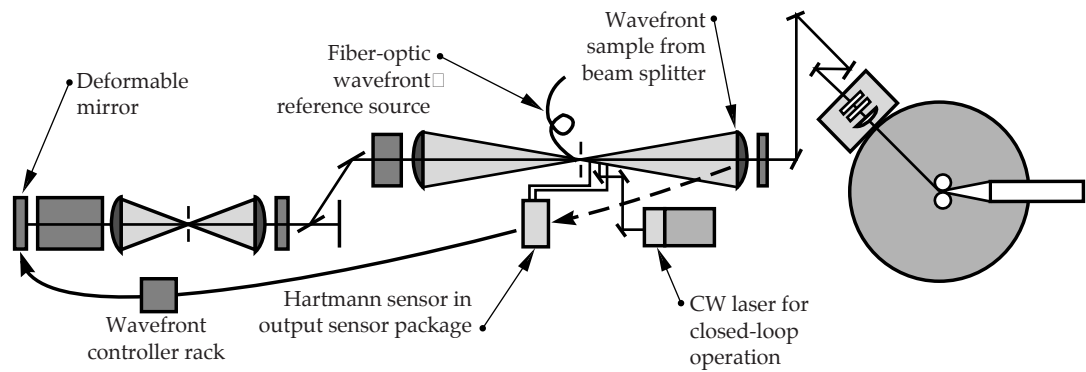
closed-loop operation is interrupted, and the Hartmann wavefront sensor is configured to measure the pulsed wavefront. The measured pulsed wavefront error provides additional information for setting precorrection wavefronts prior to the next shot.

Requirements for the system include operation at 1 Hz closed-loop bandwidth, reduction of low spatial frequency angles in the beam to less than $20 \mu\text{rad}$, and a range of at least 15 waves for correction of simple curvature measured at beamline output. Figure 19 shows the location of system components.

Hartmann Sensor

The Hartmann sensor includes a 2D array of lenslets and a CCD video camera. The output sensor (Figure 7) delivers a demagnified image of the output beam to the lenslet array. Each lenslet collects light from a specific part of the beam and focuses it on the CCD. The focal length must correspond accurately to the distance from the lenslet to the CCD; this result is obtained using an index-matching fluid sealed between the lenslets and an optical flat. The lateral position of the focused spot is a direct measure of the direction of the light entering the lenslet. Directional data from the 77 hexagonally packed lenslets of the NIF sensor are processed to determine the output wavefront with an accuracy of ≤ 0.1 wave averaged over the

FIGURE 19. General location of the primary wavefront control components—the Hartmann sensor, the deformable mirror, and the wavefront controller. A diagnostic beam splitter immediately following the spatial filter output lens provides a wavefront sampling surface. (40-00-1097-2265pb02)



lenslet spacing and a spatial resolution of 43 mm when mapped into the 400-mm beamline aperture.

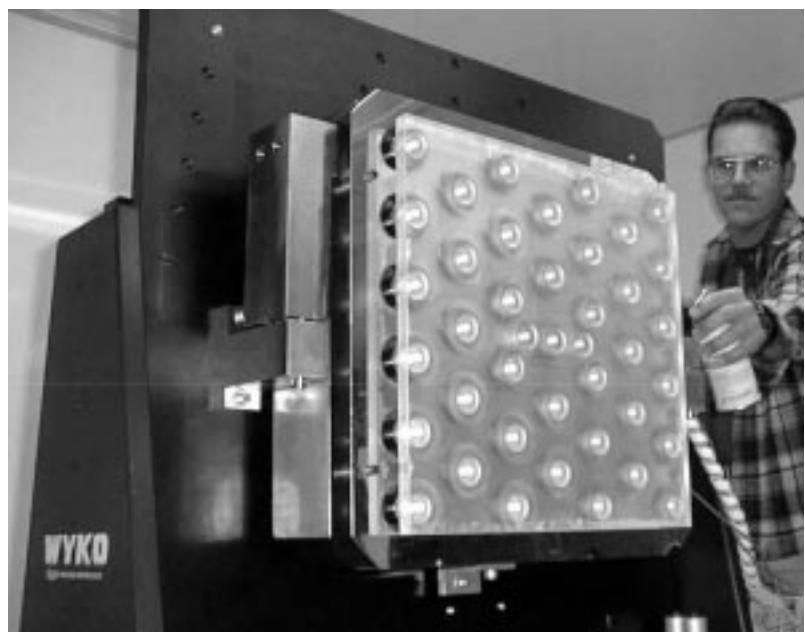
Deformable Mirror

Each NIF beam includes a large-aperture deformable mirror for wavefront control in the main laser cavity. The required optical clear aperture is approximately 400×400 mm square. The mirror shape is determined by small push and pull displacements of 39 actuators spaced 74 mm apart on the back side of the mirror. After three deformable mirror designs were built

and tested, including two from commercial sources, an LLNL design was judged to offer the best performance. Its PMN (lead magnesium niobate) actuators can be replaced in the event of failure, and the epoxy joints used to attach the actuators are protected from flashlamp light. The ceramic part of each actuator is kept under compression by preloading to minimize the growth of microcracks.

Figure 20 is a photograph of the prototype mirror built from the chosen design. It has a BK7 glass substrate with a hard dielectric coating having a reflectivity of $\geq 99.5\%$ and a 1ω transmission of $>0.2\%$.

FIGURE 20. An LLNL 40- × 40-cm prototype deformable mirror has been successfully assembled and tested. (40-00-0499-0886pb01)



The transmission is required to allow viewing of centering references located behind each mirror.

When installed in the laboratory for testing, the LLNL prototype mirror had sufficiently low residual error at nominal drive voltages that response functions were readily measured, and subsequent modeling of the deformable mirror in a NIF beamline has used the measured functions. The mirror was also operated in closed-loop mode and was able to match the nominally flat interferometer reference mirror to within $0.3\ \mu\text{m}$ peak-to-valley and $0.03\ \mu\text{m}$ rms. Subsequently, with an aberrated optic in the beam to simulate some of the general features of a NIF beamline, the closed-loop system was able to restore a flat wavefront to similar accuracy. Although additional testing will be done on the LLNL mirror, it is now considered to be NIF qualified.

Figure 21a shows the predicted long spatial-wavelength aberration of a NIF beamline resulting from a combination of thermal distortions of the amplifier slabs, inaccuracies in optics fabrication, alignment errors, optic distortions due to coating stress, and the bending of parts due to mounting and gravity effects. The properties of the focused 3ω spot that would result from such a wavefront were calculated using the extensive modeling capabilities developed for the NIF system over the last several years. The results are presented in Figures 21b and 21c. The beam

focuses very poorly, with a $37\text{-}\mu\text{rad}$ spot radius required to include 80% of the beam energy.

When a deformable mirror with the measured characteristics of the LLNL prototype mirror is included in the beamline model as part of a wavefront correction system, the mirror assumes the shape of the surface in Figure 22a, and the focus characteristics change to those presented in Figures 22b and 22c. The 80% spot radius is reduced by more than $3.5\times$ to $10.5\ \mu\text{rad}$, which means an increase in the focused fluence of more than an order of magnitude. Of course, system aberrations that have higher spatial frequencies than the deformable mirror can address will degrade this result, but the wavefront correction capability plays an essential role in achieving NIF performance goals.

Wavefront Controller

The wavefront controller function is accomplished by systems that are modular at the eight-beam-bundle level. Each wavefront controller comprises computer hardware and software to periodically calibrate the associated Hartmann wavefront sensors and deformable mirrors, operate the automatic wavefront correction loops during preparations for a shot, and capture pulsed wavefront measurement data during a shot. In the moments immediately prior to a shot, the system is generally operated under closed-loop control to an

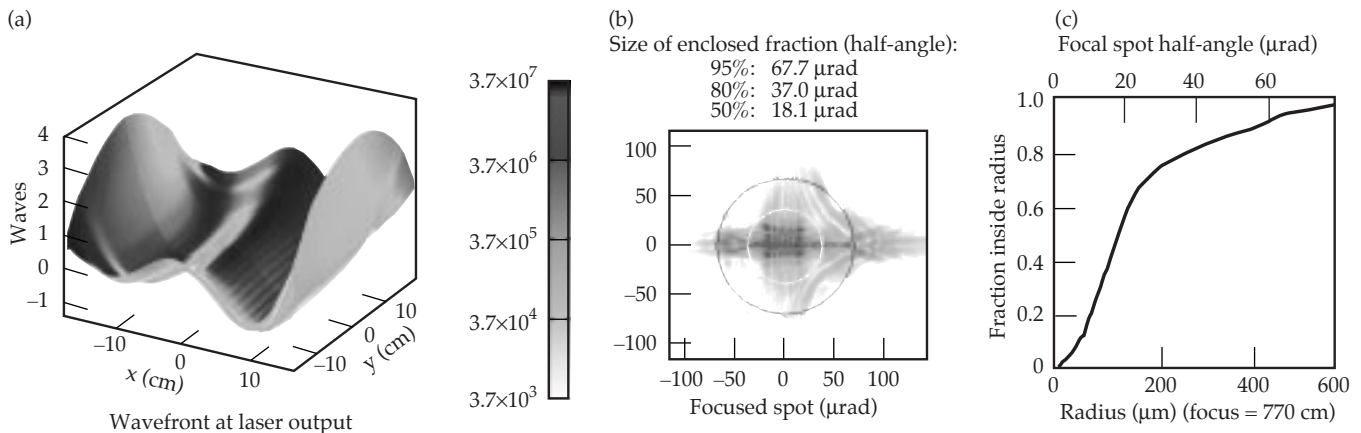


FIGURE 21. Performance of a NIF beamline is degraded by optical aberrations: (a) uncorrected output wavefront, (b) focal spot corresponding to these aberrations, and (c) radial distribution of energy. (40-00-0499-0884pb01)

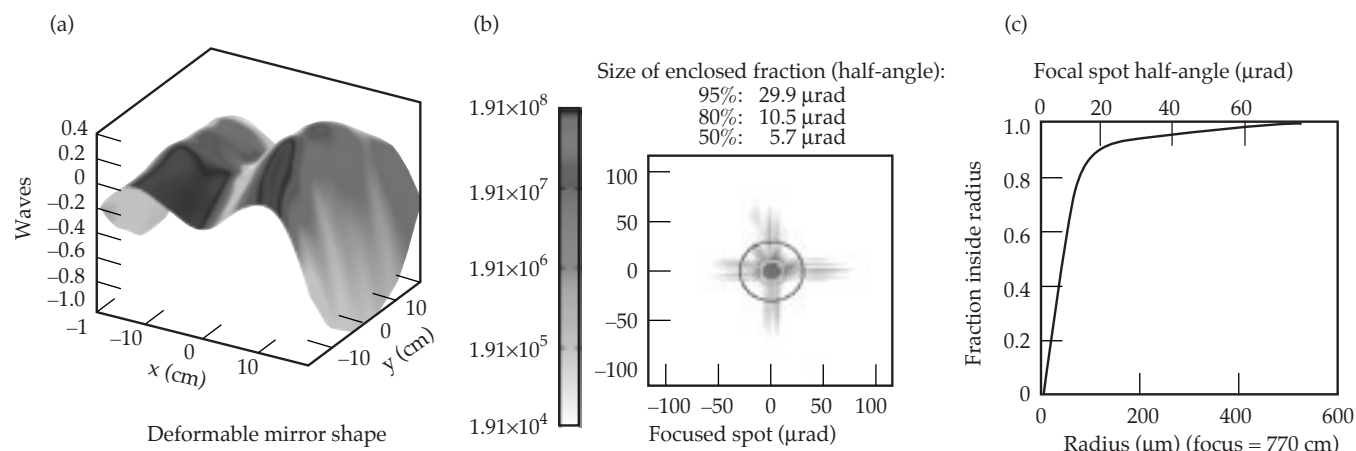


FIGURE 22. Performance of a NIF beamline when the wavefront correction system is in operation: (a) shape of the deformable mirror, (b) improved focal spot, and (c) radial distribution of energy. (40-00-0499-0885pb01)

offset wavefront value. This is because the flashlamp-pumped amplifiers introduce a dynamic wavefront change when they are fired, and the wavefront system must be set to anticipate that change.

Since the Hartmann sensor data is in video format, the controller incorporates image processing capabilities appropriate for recognizing and tracking the position of the 77 focused spots from each Hartmann image. The image processing code attains maximum accuracy by automatic adjustment of software parameters for gray scale and brightness. The controller also measures and applies the influence matrix for the deformable mirror actuators and the amplifier pre-correction file in accordance with the mirror control algorithm. When operating in closed-loop, the controller is intended to maintain a closed-loop bandwidth of approximately 1 Hz on each beam.

The NIF wavefront controller hardware will use the VME industrial computer bus and multiprocessor architecture, which is designed to make maximum use of standard components and to accommodate replacement of modular elements as microprocessors and other computer electronics continue to evolve. The system will be attached to the integrated computer control system network using CORBA (see p. 21).

Summary

All of the laser control systems have completed 100% design reviews, and we are proceeding with prototype testing, Title III design, and procurement. Activities are now shifting to completion of detailed drawings and ordering of production hardware. As this hardware arrives, it will be thoroughly tested before installation in the laser, switchyard, and target bays of the NIF facility. The beam control and laser diagnostics systems will be among the first to be activated so that their functionality can be used to control and monitor subsequent additions to each beamline. When NIF is completed, these systems will operate in conjunction with the integrated computer controls to provide the level of automatic operation that is essential for successful facility operation.

Acknowledgments

The authors specifically acknowledge the significant contributions of the talented technology associates, technicians, and designers in beam control and laser diagnostics to the designs described above. In addition, because the NIF Project is now in its fifth year, the design has benefited from the efforts of some who are no longer on the staff, but whose contributions are not forgotten.

Notes and References

1. Present baseline design uses a tapered cone on Pass #4 only preventing pinhole closure for a 20-ns pulse. Passes #1, #2, and #3 use stainless-steel washer-type pinholes.
2. The CSF pinhole wheel rotates to multiple precision set points to locate an alignment reticle, a selection of the shot pinholes, several optics inspection pinholes, or a 35-mm clear aperture.
3. The TSF pinhole wheel positions multiple shot pinholes or an 80-mm clear aperture.
4. Two insertable light sources mounted on a common translation stage provide references for beam alignment and wavefront calibration.
5. Insertable 45° reflector with attached dump for 3 ω diagnostic beam is withdrawn from beam for alignment and optical inspection.

